Proposition for the EUSIPCO 2025 Phased Array Signal Processing Student Challenge

Julien Lesouple
Université de Toulouse
ENAC

Alexandre Brochard
Université de Toulouse
ISAE-SUPAERO/ENAC

Lorenzo Ortega
IPSA/TéSA

Paul Thevenon
Université de Toulouse
ENAC

Evelyn Lisseth Rojano Fernández
Université de Toulouse
CNES/ENAC

***Abstract*—Global Navigation Satellite Systems rely on estimating the signal propagation delay and Doppler shift to a set of visible satellites, which in turn allows to determine the receiver position, velocity and timing. However, the presence of interfering signals degrades the estimation of such synchronization parameters, reason why robust solutions must be accounted for. One specific kind of interference are jamming, where a powerful signal is emitted in the same bandwidth as the signal of interest. One possible way to mitigate jamming is to resort to an antenna array. Doing so, spatial diversity can help to estimate the most powerful signal, allegedly the interference, and perform detection, localization and mitigation. In our solution, we propose two methods: the first one is an offline one, which uses snapshots where the interference is the most powerful to allow for precise detection and localization of the interferer. The other one is an online one, allowing to perform detection, localization and mitigation in real time of the interfering signal.**

***Keywords*—beamforming, jamming, GNSS.**

I. Introduction

Global Navigation Satellite System (GNSS) are known to be vulnerable to a wide range variety of non-nominal propagation conditions, threats and attacks, with interference sources, whether intentional or unintentional, playing a major role [1]–[3]. In safety-critical applications, effective interference mitigation is therefore essential to ensure reliable positioning. This vulnerability is largely due to the extremely low received power of GNSS signals, typically around -159 dBW [4], which place them below the noise floor and makes them highly susceptible to disruption.

In the context of antenna array receivers, interference mitigation benefits from spatial diversity, which enables not only the identification and localization of interference sources, but also their mitigation [5]. State-of-the-art techniques in this area include beamforming, spatial filtering, and adaptive null steering [6], which aim to enhance the desired signal while attenuating interference arriving from specific directions. These spatial processing methods complement the temporal and spectral approaches used in single antenna systems.

We propose to use beamforming and Direction Of Arrival (DOA) estimation techniques to detect, localize, and mitigate jamming signals. Our strategy involves two complementary approaches: an online method and an offline one. The primary goal is to develop an online algorithm capable of performing real-time detection, localization, and mitigation of the jamming signal, emulating a commercial implementation. The offline method is employed to perform a more precise detection and localization of the interference.

The article is organized as follows: Sec. II presents the antenna array used and the corresponding signal model, Sec. III presents some state of the art array processing methods along with the two proposed approaches. Finally, Sec. IV presents the results on the challenge dataset while Sec. V concludes this proposition.

II. Signal model and array configuration

We consider an array of $L = 4$ antennas arranged in a square with side length $d = 10$ cm. A local coordinate system is defined such that its origin lies at the center of the square, with the xy-plane aligned with the antenna plane and the z-axis pointing outward, normal to the array. We assume that all incoming signals originate from far-field sources, such that the wavefronts impinging on the array can be approximated as planar. For each source, we denote $\phi \in \left[0, \frac{\pi}{2}\right)$ as the elevation and $\theta \in [-\pi, \pi)$ as the azimuth. Note that all these definitions were specified by the challenge (including the left hand rule frame). We denote $s(t)$ the signal received at the origin, while the signal received at antenna n is denoted by $s(t - \tau_n)$. All these notations are illustrated in Fig. 1.

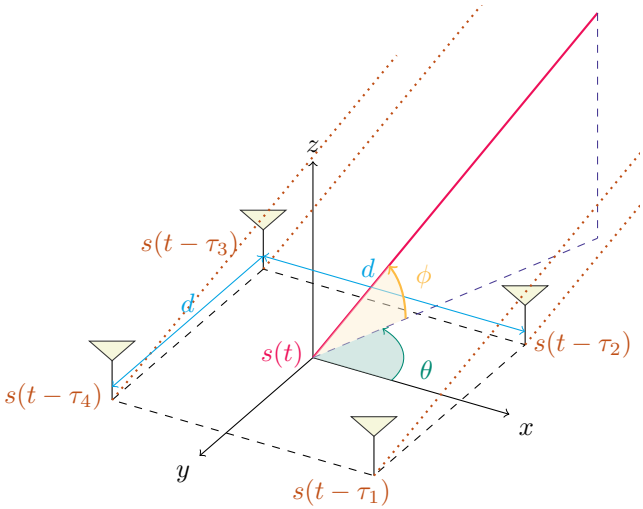

Fig. 1: Schematic of the problem with $\theta < 0$.

A. Single signal reception scenario

For a single signal impinging a calibrated square array of 4 antennas after demodulation around frequency f_c, the snapshot vector can be expressed as

$$\boldsymbol{y}(t) \triangleq \begin{bmatrix} y_1(t) \\ y_2(t) \\ y_3(t) \\ y_4(t) \end{bmatrix} = \begin{bmatrix} s(t-\tau_1) + n_1(t) \\ s(t-\tau_2) + n_2(t) \\ s(t-\tau_3) + n_3(t) \\ s(t-\tau_4) + n_4(t) \end{bmatrix} = \begin{bmatrix} s(t-\tau_1) \\ s(t-\tau_2) \\ s(t-\tau_3) \\ s(t-\tau_4) \end{bmatrix} + \boldsymbol{n}(t), \tag{1}$$

with $\boldsymbol{n}(t) \sim \mathcal{CN}(\boldsymbol{0}, \sigma^2 \boldsymbol{I}_4)$ the noise, where σ^2 denotes the noise variance at each antenna element. Assuming a narrow-band signal around the carrier frequency f_c with baseband signal $s(t)$, and considering short delays relative to the wavelength $\lambda_c = \frac{c}{f_c}$, we have[1]

$$s(t-\tau_n) \approx s(t) e^{j \boldsymbol{k}^T \boldsymbol{r}_n} \tag{2}$$

with antenna positions and wave vector

$$\mathbf{R} = \frac{d}{2} \begin{bmatrix} 1 & 1 & -1 & -1 \\ 1 & -1 & -1 & 1 \\ 0 & 0 & 0 & 0 \end{bmatrix}, \quad \boldsymbol{k} = \frac{2\pi}{\lambda} \begin{bmatrix} \cos\phi \cos\theta \\ \cos\phi \sin\theta \\ \sin\phi \end{bmatrix}, \tag{3}$$

where each column $\boldsymbol{r}_n$ corresponds to the position vector of the n-th antenna. Therefore, we have

$$\boldsymbol{y}(t) = \boldsymbol{a}(\theta, \phi) s(t) + \boldsymbol{n}(t), \tag{4}$$

with

$$\boldsymbol{a}(\theta, \phi) = \begin{bmatrix} \exp\left(j \frac{\pi d \sqrt{2}}{\lambda_c} \cos(\phi) \cos(\theta - \frac{\pi}{4}) \right) \\ \exp\left(j \frac{\pi d \sqrt{2}}{\lambda_c} \cos(\phi) \cos(\theta + \frac{\pi}{4}) \right) \\ \exp\left(j \frac{\pi d \sqrt{2}}{\lambda_c} \cos(\phi) \cos(\theta + \frac{3\pi}{4}) \right) \\ \exp\left(j \frac{\pi d \sqrt{2}}{\lambda_c} \cos(\phi) \cos(\theta - \frac{3\pi}{4}) \right) \end{bmatrix} \tag{5}$$

the steering vector in direction (θ, ϕ). Note that according to [7, Eq. (4.157)], we should have $d \leq \frac{\lambda_c}{2}$ to avoid ambiguous DOA estimation, which is not satisfied here.

B. Multiple signal reception scenario

When P signals arrive at the array, Eq. (4) becomes

$$\boldsymbol{y}(t) = \sum_{p=1}^{P} s_p(t) \boldsymbol{a}(\theta_p, \phi_p) + \boldsymbol{n}(t) = \boldsymbol{A}(\boldsymbol{\theta}, \boldsymbol{\phi}) \boldsymbol{s}(t) + \boldsymbol{n}(t), \tag{6}$$

where $\boldsymbol{a}(\theta_p, \phi_p)$ is the steering vector associated with the p-th source arriving from elevation θ_p, and azimuth ϕ_p (as defined in Fig. 1). In the matrix form, $\boldsymbol{A}(\boldsymbol{\theta}, \boldsymbol{\phi}) = \begin{bmatrix} \boldsymbol{a}(\theta_1, \phi_1) & \cdots & \boldsymbol{a}(\theta_P, \phi_P) \end{bmatrix} \in \mathbb{C}^{L \times P}$, $\boldsymbol{\theta} = \begin{bmatrix} \theta_1 & \cdots & \theta_P \end{bmatrix}^T$, $\boldsymbol{\phi} = \begin{bmatrix} \phi_1 & \cdots & \phi_P \end{bmatrix}^T$, $\boldsymbol{s}(t) = \begin{bmatrix} s_1(t) & \cdots & s_P(t) \end{bmatrix}^T$, and $\boldsymbol{n}(t)$ is the same as before.

One special case is when the sources $s_p(t)$ are considered centered complex Gaussian with covariance matrix $\boldsymbol{R}_s$. In that case, the snapshot is also complex centered Gaussian with covariance matrix

$$\boldsymbol{R}_y = \boldsymbol{A}(\boldsymbol{\theta}, \boldsymbol{\phi}) \boldsymbol{R}_s \boldsymbol{A}^H(\boldsymbol{\theta}, \boldsymbol{\phi}) + \sigma^2 \boldsymbol{I}_4. \tag{7}$$

[1]For a right hand rule frame, a minus sign is expected in the exponential.

When the sources are uncorrelated, the matrix $\boldsymbol{R}_s$ becomes diagonal where the p-th diagonal term P_p is the power of the signal p, leading

$$\boldsymbol{R}_y = \sum_{p=1}^{P} P_p \boldsymbol{a}(\theta_p, \phi_p) \boldsymbol{a}^H(\theta_p, \phi_p) + \sigma^2 \boldsymbol{I}_4. \tag{8}$$

If $P < 4$ and the steering vectors are independent, the summation is of rank P. An eigenvalue decomposition ($\lambda_1 \geq \cdots \geq \lambda_P$) in an orthonormal family $\boldsymbol{U}_s$ and completed with $\boldsymbol{U}_n$ into an orthonormal basis of $\mathbb{C}^4$ leads

$$\begin{aligned} \boldsymbol{R}_y &= \boldsymbol{U}_s \boldsymbol{\Lambda}_s \boldsymbol{U}_s^H + \sigma^2 \begin{bmatrix} \boldsymbol{U}_s & \boldsymbol{U}_n \end{bmatrix} \begin{bmatrix} \boldsymbol{U}_s^H \\ \boldsymbol{U}_n^H \end{bmatrix} \\ &= \boldsymbol{U}_s \boldsymbol{\Lambda}_s' \boldsymbol{U}_s^H + \sigma^2 \boldsymbol{U}_n \boldsymbol{U}_n^H, \end{aligned} \tag{9}$$

with $\boldsymbol{\Lambda}_s' = \boldsymbol{\Lambda}_s + \sigma^2 \boldsymbol{I}$ and $\boldsymbol{\Lambda}_s = \mathrm{diag}(\lambda_1, \cdots, \lambda_P)$.

C. Observation model

The received signal is sampled by an analog-to-digital converter (ADC) operating at a sampling frequency F_s, with sampling period T_s. We consider an observation window of duration T_i, leading to a total of $K = \lfloor T_i / T_s \rfloor$ samples. This yields to the following discrete-time signal model

$$\boldsymbol{Y} = \boldsymbol{A}(\boldsymbol{\theta}, \boldsymbol{\phi}) \boldsymbol{S} + \boldsymbol{N} \in \mathbb{C}^{L \times K}, \tag{10}$$

where $\boldsymbol{Y} = \begin{bmatrix} \boldsymbol{y}(T_s), & \cdots & , \boldsymbol{y}(KT_s) \end{bmatrix} \in \mathbb{C}^{L \times K}$ gathers all the snapshots, $\boldsymbol{S} = \begin{bmatrix} \boldsymbol{s}(T_s), & \cdots & , \boldsymbol{s}(KT_s) \end{bmatrix} \in \mathbb{C}^{P \times K}$ gathers the baseband signals, and $\boldsymbol{N} = \begin{bmatrix} \boldsymbol{n}(T_s), & \cdots & , \boldsymbol{n}(KT_s) \end{bmatrix} \in \mathbb{C}^{L \times K}$ denotes the noise samples.

III. Array processing techniques

Array processing provides an additional (spatial) dimension allowing to perform two main tasks: DOA estimation and spatial filtering (beamforming).

A. DOA estimation

One of the most famous methods for DOA estimation is the MUltiple SIgnal Classification (MUSIC) algorithm [8]. MUSIC is a subspace-based technique that exploits the eigenvectors of the snapshot covariance matrix $\boldsymbol{R}_y$ in the case of uncorrelated centered sources to separate the signal and noise subspaces. In that case, the covariance matrix is expressed as in (9) and the key idea is that the steering vectors of the incoming signals lie in the signal subspace $\boldsymbol{U}_s$, which is orthogonal to the noise subspace $\boldsymbol{U}_n$. By scanning all possible directions and computing a pseudo-spectrum function, MUSIC identifies peaks corresponding to the true signal directions. The MUSIC pseudo-spectrum is defined as:

$$P_{\text{MUSIC}}(\theta, \phi) = \frac{1}{\boldsymbol{a}^H(\theta, \phi) \boldsymbol{U}_n \boldsymbol{U}_n^H \boldsymbol{a}(\theta, \phi)}. \tag{11}$$

In practice, the covariance matrix $\boldsymbol{R}_y$ is unknown and must be estimated from the data, and the corresponding subspaces $\hat{\boldsymbol{U}}_s$ and $\hat{\boldsymbol{U}}_n$ are obtained with an eigenvalue decomposition. A natural choice is to resort to the sample covariance matrix

$$\hat{\boldsymbol{R}}_y \triangleq \frac{1}{K} \sum_{k=1}^{K} \boldsymbol{y}(kT_s) \boldsymbol{y}(kT_s)^H = \frac{1}{K} \boldsymbol{Y} \boldsymbol{Y}^H. \tag{12}$$

In our case, the snapshots lies in a 4D space and therefore P cannot exceed 4, which is not the case due to all the GNSS signals. To simplify, we will consider that the interfering signal has higher power than the GNSS signals, and therefore take $P = 1$ and estimate a single DOA assumed to be the interferer. Indeed, in the GNSS context, although multiple GNSS signals are simultaneously received by the antenna array, their spread-spectrum structure (based on PRN codes) and their power being typically below the noise floor cause them to appear as background noise from the perspective of array processing algorithms such as MUSIC. The use of the sample covariance matrix could increase this power due to the autocorrelation properties of GNSS signals, but we have remarked in our experiments that taking into account or not this correlation did not change the output of the DOA estimation.

B. Beamforming

Among spatial filtering techniques, beamforming provides an effective way to enhance signals from desired directions while suppressing interferences such as jamming. Beamforming operates by applying spatial weights $\boldsymbol{w}$ to the observations $\boldsymbol{Y}$, resulting in an output signal

$$\boldsymbol{y}_{BF} = \boldsymbol{w}^H \boldsymbol{Y}. \tag{13}$$

In conventional beamforming (CBF), the weights are aligned with the steering vector $\boldsymbol{w} = \boldsymbol{a}(\theta_0, \phi_0)$ to enhance the reception in the desired direction (θ_0, ϕ_0). However, this method does not try to attenuate other signals. Adaptive beamformers, such as the Minimum Power Distortionless Response (MPDR) [7, Chap. 6.2.4], allow to point in a direction while attenuating others. The MPDR minimizes the output power while preserving the signal arriving from the specific direction. The MPDR weights are obtained by solving the following constrained optimization problem:

$$\boldsymbol{w}_{\text{MPDR}} = \arg\min_{\boldsymbol{w}} \mathbb{E}\left[\left|\boldsymbol{w}^H \boldsymbol{y}(t)\right|^2\right] = \boldsymbol{w}^H \boldsymbol{R}_y \boldsymbol{w} \tag{14}$$

$$\text{s.t} \quad \boldsymbol{w}^H \boldsymbol{a}(\theta_0, \phi_0) = 1, \tag{15}$$

leading to

$$\boldsymbol{w}_{\text{MPDR}} = \frac{\boldsymbol{R}_y^{-1} \boldsymbol{a}(\theta_0, \phi_0)}{\boldsymbol{a}^H(\theta_0, \phi_0) \boldsymbol{R}_y^{-1} \boldsymbol{a}(\theta_0, \phi_0)}. \tag{16}$$

By leveraging the spatial information encapsulated in $\boldsymbol{R}_y$, the MPDR automatically place nulls in the directions of the interference sources while preserving gain in the direction of interest. Once again, this matrix is not known in practice and we use the sample covariance matrix.

C. Proposed approaches

The jamming power has been observed to be increasing with respect to time in that experiment. We propose two approaches. The first one is *offline* and estimates the DOA of the interference using MUSIC on the last samples of data, where it is the most powerful. This estimated DOA is then used to implement an MPDR beamformer in the corresponding direction. This filtered data is expected to help us detect when the interference begins. Then, we propose an *online* method, that performs MUSIC in a continuous fashion to estimate the interference DOA with respect to time. In parallel, we implement an MPDR towards the zenith ($\phi_0 = \frac{\pi}{2}$). This is the most natural direction to look at as the array is horizontal. The filtered data are then fed to a GNSS engine[2] to compute PVT under various configurations, and are also used to perform detection of the interfering signal.

IV. Results

A. Offline proposition

We use the last 5 seconds of data to perform MUSIC iteratively on θ and ϕ with a refined grid on the second iteration to estimate the interference DOA. Results are visible in Fig. 2.

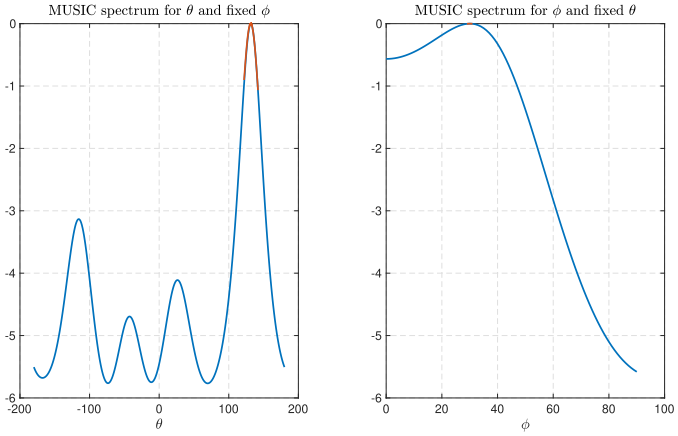

Fig. 2: MUSIC spectra for ϕ and θ.

The corresponding estimated DOA is then $\phi = 30.1°$, $\theta = 131.5°$. We acknowledge that a 30° elevation value is too high. Our best explanation is that the array lacks calibration and therefore the expression of the steering vector (5) is not realistic. Another explanation would be the the non-respect of the condition $d \leq \frac{\lambda_c}{2}$ and/or the presence of more than 4 sources lead to aliasing in the spectrum. Although the angle estimation is not correct, the corresponding interference subspace does not depend on this estimate and this should not affect the detection and the online method proposed in the next section.

Next, we use this estimated DOA (and interference subspace) to steer the array toward the interference and detect when it starts. To do so, we split the data into 1 s non overlapping windows and implement an MPDR beamformer on them. Then, we look at the power of the filtered observations, i.e., $\sum_{t\in\text{window}} |\boldsymbol{w}_{\text{MPDR}}^H \boldsymbol{y}(t)|^2$. We compare this statistic to the norm of the non filtered signals $\sum_{t\in\text{window}} \|\boldsymbol{Y}(t)\|_2^2$ to appreciate the benefits of the beamforming. The results are depicted in Figs 3 and 4. We clearly see the effects of the jammer on the two plots. However, it seems clearer on the right plot (after MPDR) that jamming starts at 106 s. Note that we also notice a small peak around 18 s.

[2]https://gnss-sdr.org/

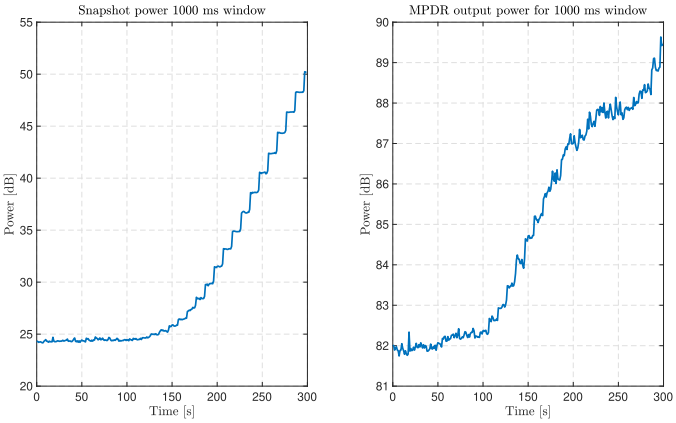

Fig. 3: Comparison of signal power at input and output of the offline MPDR.

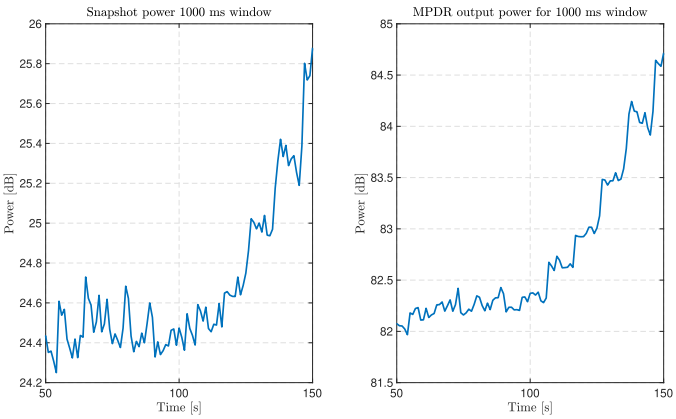

Fig. 4: Comparison of signal power at input and output of the offline MPDR (zoomed).

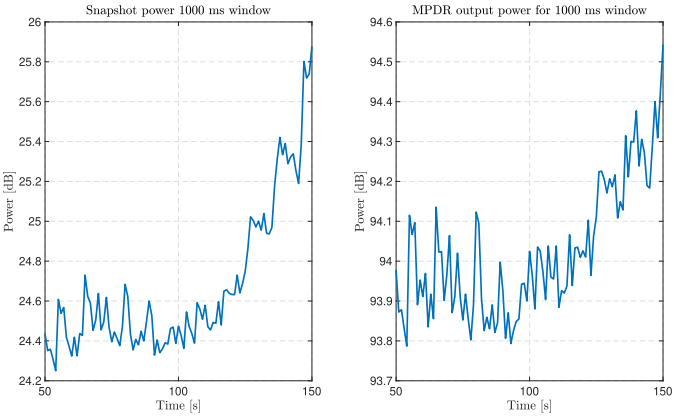

Fig. 5: Comparison of signal power at input and output of the online MPDR (zoomed).

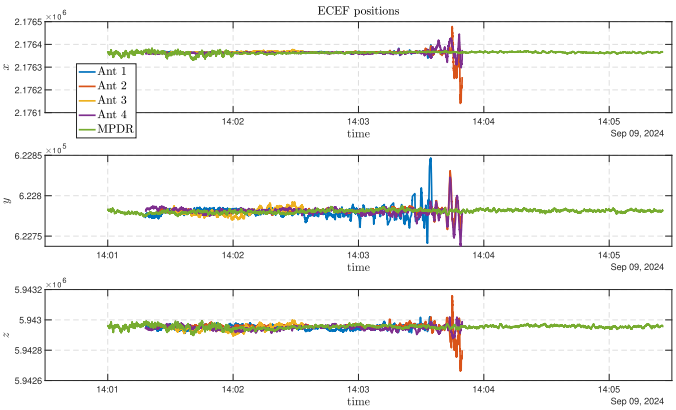

Fig. 6: Comparison of (x, y, z) coordinates in ECEF frame with and without beamforming.

B. Online

Now, we use an MPDR steer toward the zenith of the array. We are again able to plot the output power versus time to try to detect the jamming. The results are shown in Fig. 5. We can see that detection appears later now (around 125 s) and there are no advantage compared to the input power.

Nevertheless, the MPDR allows us to filter the data before feeding them to a PVT engine. We compare the ECEF positions using GPS L1 C/A signals of the single antennas and the ones obtained with the filtered observations in Fig. 6. As observed in this figure, the position determined by the MPDR method exhibits the greatest stability. The solutions computed for each individual antenna are interrupted at some point after the start of the interference. On the other hand, the solution using the MPDR technique continues to be available after the start of the interference without being disturbed by it: the mean and standard deviation of the estimated position remain the same as before the interference. This results shows that the MPDR is able to mitigate well the jammer without any prior information about it.

A similar result is observed in Fig. 7 where we added comparison to Galileo E1B and the GPS+Galileo solution. The greatest stability is achieved through the use of multi-constellation systems, although GPS and Galileo individually yield accurate results. The PVT positions for this solution are presented in Fig. 8 where the mean latitude for GPS+Galileo is $69°16'32"$, longitude is $15°58'84"$, and height is 43.23 m.

On an other hand, we also apply MUSIC all along the experiment. We chose to fix $\phi = 0$ in the spectrum evaluation to focus on the azimuth of the interference. We obtain the spectrogram depicted in Fig. 9 and the corresponding estimates are plotted in Fig. 10. The estimate converges to the one of the offline method. We have low confidence on these estimated for the same reasons mentioned in the offline results.

V. Conclusion

In this study, we analyzed a dataset comprising GNSS signal samples that were subjected to interference from a noise-like jammer with increasing power over time. We proposed various approaches based on array processing techniques to meet the objectives of this challenge. Specifically, we introduced two methods: an “offline” approach, where we examined specific segments of the dataset to extract relevant information, and an “online” approach, where we applied an MPDR beamformer toward the azimuth of the local frame of the antennas.

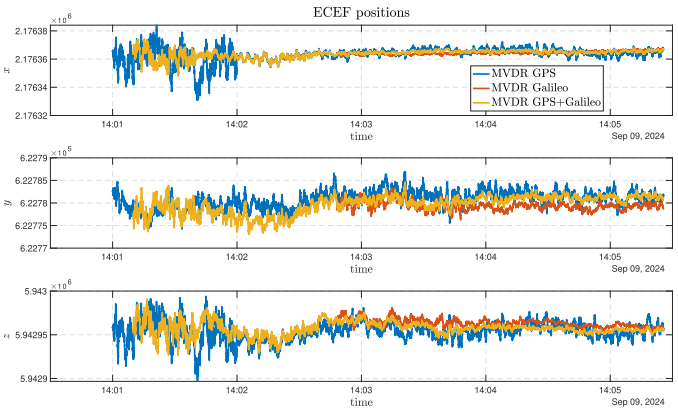

Fig. 7: Comparison of (x, y, z) coordinates in ECEF frame with beamforming for multiple constellation.

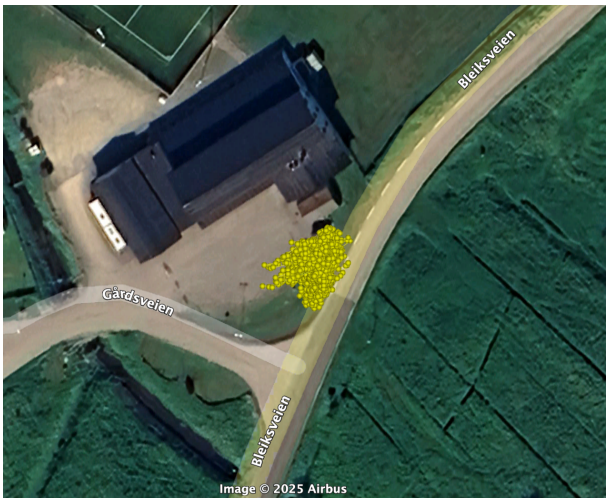

Fig. 8: PVT of the GPS+Galileo and MPDR solution (Google Earth).

Through our analysis, we successfully detected the onset of jamming around 106 seconds, marked by an increase in power. Additionally, we estimated the DOA of the jammer using the MUSIC algorithm, yielding the coordinates $\phi = 30.1°$ and $\theta = 131.5°$. Finally, we effectively mitigated the jammer by applying the MPDR beamformer to the azimuth of the local frame of the antennas.

All the objectives were accomplished using fundamental array processing techniques. However, there are avenues for further improvements. For instance, the knowledge of the emitted signals (PRN codes) or the knowledge of the known GNSS emitter solutions could be used to develop other beamformers taking into account these informations.

References

[1] M. G. Amin, P. Closas, A. Broumandan, and J. L. Volakis, "Vulnerabilities, Threats, and Authentication in Satellite-based Navigation Systems [scanning the issue]," *Proceedings of the IEEE*, vol. 104, no. 6, pp. 1169–1173, June 2016.

[2] F. Dovis, *GNSS Interference Threats & Countermeasures*. Artech House, 2015.

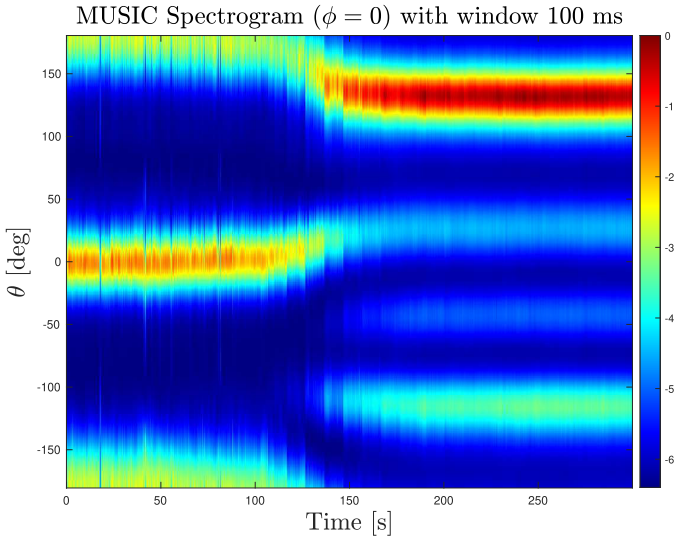

Fig. 9: MUSIC spectrogram for $\phi = 0$.

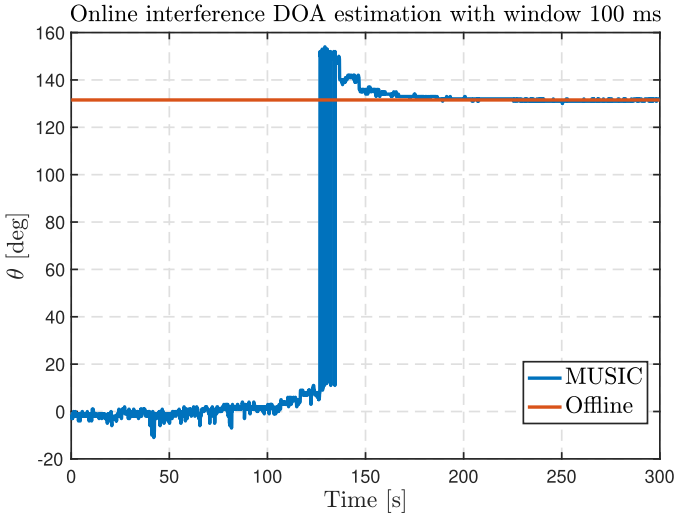

Fig. 10: Estimated DOA with MUSIC for $\phi = 0$.

[3] P. Closas, L. Ortega, J. Lesouple, and P. Djurić, "Emerging trends in signal processing and machine learning for positioning, navigation and timing information: special issue editorial," *EURASIP Journal on Advances in Signal Processing*, vol. 2024, no. 1, p. 84, 2024. [Online]. Available: https://doi.org/10.1186/s13634-024-01182-8

[4] E. Kaplan and C. Hegarty, *Understanding GPS: Principles And Applications*, 11 2005.

[5] C. Fernández-Prades, J. Arribas, and P. Closas, "Robust GNSS receivers by array signal processing: Theory and implementation," *Proceedings of the IEEE*, vol. 104, no. 6, pp. 1207–1220, June 2016.

[6] P. Closas, C. Fernandez-Prades, and J. Arribas, "Multi-antenna techniques for interference mitigation in gnss signal acquisition," *EURASIP Journal on Advances in Signal Processing*, 2013.

[7] H. L. Van Trees, *Optimum Array Processing*. Wiley-Interscience, New-York, 2002.

[8] R. Schmidt, "Multiple emitter location and signal parameter estimation," *IEEE Trans. Antennas Propag.*, vol. 34, no. 3, pp. 276–280, 1986.